Molecular Diversity (2023) 27:1735–1749
https://doi.org/10.1007/s11030-022-10527-0

ORIGINAL ARTICLE

Novel bis-ureido-substituted sulfaguanidines and sulfisoxazoles as carbonic anhydrase and acetylcholinesterase inhibitors

Nebih Lolak[1] · Süleyman Akocak[1] · Mustafa Durgun[2] · Hatice Esra Duran[3] · Adem Necip[4] · Cüneyt Türkeş[5] · Mesut Işık[6] · Şükrü Beydemir[7,8]

Received: 2 May 2022 / Accepted: 9 September 2022 / Published online: 22 September 2022

Abstract

To discover alternative substances to compounds used to treat many diseases, especially treating Alzheimer's disease (AD) and Parkinson's disease targeting carbonic anhydrase (*h*CA) and acetylcholinesterase (AChE) enzymes, is important. For this purpose, a series of novel bis-ureido-substituted sulfaguanidine (**SG1–4**) and sulfisoxazole (**SO1–4**) derivatives were synthesized, and their inhibitory capacities were screened against *h*CA isoenzymes (*h*CA I and II) and AChE. Possible binding mechanisms of inhibitors to the active site were elucidated by in silico studies, and the results were supported by in vitro results. Moreover, the percent radical scavenging capacities of the derivatives were also evaluated. The derivatives (**SG1–4** and **SO1–4**) were more effective against *h*CAs compared to standard drug acetazolamide (K_I values of 98.28–439.17 nM for *h*CA I and II, respectively) and exhibited the highest inhibition with the K_Is in the ranges of 2.54 ± 0.50–41.02 ± 7.52 nM for *h*CA I, 11.20 ± 2.97–67.14 ± 13.58 nM for *h*CA II, and 257.60 ± 27.84–442.60 ± 52.13 nM for AChE. Also, compounds **SG1** and **SO1** also showed ABTS radical scavenging activity at the rate of 70% and 78%, respectively. These results will contribute to the literature for the rational design and synthesis of new potent and selective inhibitors targeting *h*CAs and AChE with multifunctional effects such as radical scavenging as well as inhibition.

Graphical abstract

This study focused on the synthesis and inhibitory effects of bis-ureido-substituted sulfaguanidine (**SG1–4**) andsulfisoxazole (**SO1–4**) derivatives against human hCA I and II isoforms and AChE. In order to test synthesizedderivatives' free radical scavenging potentials were the DPPH and ABTS assays. In silico studies elucidatedpossible binding mechanisms of inhibitors to the active site.

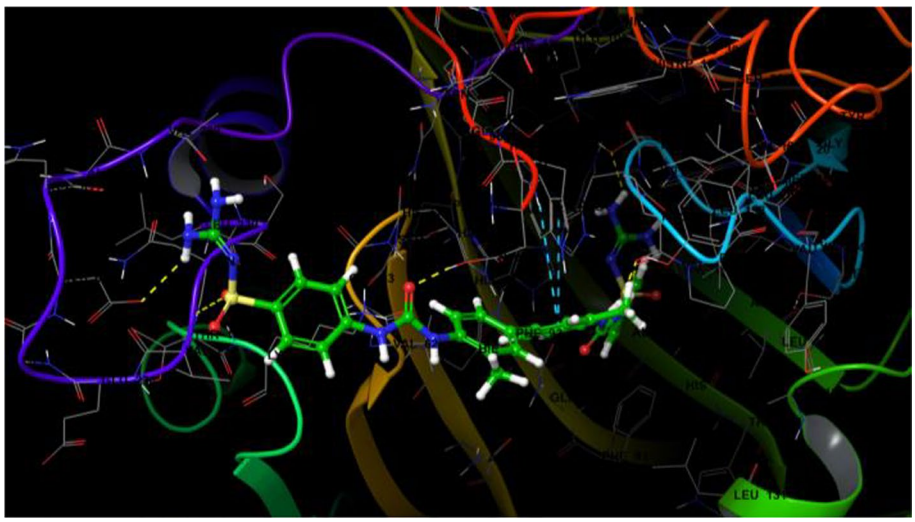

Extended author information available on the last page of the article

Keywords Carbonic anhydrase · Acetylcholinesterase · Molecular docking · Sulfaguanidine · Sulfisoxazole

Introduction

Alzheimer's disease (AD) is common, especially in older adults, due to metabolic damage in different biochemical pathways. There are different strategies for treating this disease, and one of the most effective is the "cholinergic hypothesis." According to this hypothesis, AD treatment can increase the neurotransmitter acetylcholine level in the presynaptic space or prevent their decrease [1–3]. The neurotransmitter acetylcholine, playing a role in signal transfer, is catalyzed by acetylcholinesterase (AChE, EC 3.1.1.7) and converted to choline and acetyl groups. These groups are converted back to acetylcholine, catalyzed by choline acetyltransferase. The molecular basis of the therapeutic strategy of AD drugs used so far is their use as AChE inhibitors (AChEIs) [2, 4]. These inhibitors are known to be effective in treating AD and Parkinson's disease, dementia, myasthenia gravis, and ataxia associated with cholinergic deficiency. However, few of the inhibitors have been approved. Many drugs have short half-lives and peripheral cholinergic side effects that significantly limit their use [5, 6]. Consequently, there is constant research on the design and development of new drugs.

According to the amyloid cascade hypothesis, which is one of the crucial hypotheses in elucidating the molecular mechanism of AD, it is thought that β-Amiloid (Aβ) peptides formation initiates the pathogenesis of the disease [7]. The Aβ peptides found in senile plaques in the AD brain can induce these inflammatory processes in which radical oxygen species (ROS) are present [8, 9]. Excess ROS causes damage to cellular components. Oxidative stress occurs when the endogenous antioxidant defense system does not sufficiently remove them. This case is one of the leading causes of many diseases. In addition, free radicals constantly produced in the body cause oxidation of biomolecules such as DNA, protein, and lipids, which have essential vital functions, leading to cell damage and death. In this context, free radicals have been associated with various diseases, including aging, Alzheimer's, diabetes, cancer, epilepsy, ischemic, and cardiovascular disease [10–13]. Compounds with antioxidant properties that play a role in removing the cellular free radicals reduce oxidative damage and help prevent mutagenesis, carcinogenesis, and aging [14–16].

The carbonic anhydrases (CAs, EC 4.2.1.1) are a family of zinc-containing metalloenzymes found in algae, protozoa, vertebrates, some bacteria, and the cytoplasm of green plants. The enzyme plays a vital role in physiological events such as carbon dioxide and bicarbonate transport processes with reversible hydration ($CO_2 + H_2O \leftrightarrow HCO_3^- + H^+$), pH balancing, electrolyte secretion, CO_2 homeostasis, lipogenesis, urea cycle, respiration, and biosynthetic reactions [17, 18]. Seven independent gene families encode the CA isoenzymes: α-, β-, γ-, δ-, ζ-, η-, and θ-CAs. The α-CA isoforms differ significantly in their localization and distribution in tissues. The α-CA enzyme has 16 isoenzymes: cytoplasmic (CA I, II, III, VII, and XIII), mitochondrial (CA VA and VB), secretory (CA VI), membrane-bound (CA IV, IX, XII, and XIV), and non-catalytic (CA VIII, X, and XI). CA II is one of the most active isoenzymes that catalyze carbon dioxide. It is mainly found in red blood cells, lungs, kidneys, eyes, and many secretory tissues [17, 18]. Other CA isoforms are found in many tissues where they participate in biological processes such as bone resorption, lipogenesis, carbon dioxide, ion transport, acid–base balance, respiration, and electrolyte secretion. The high and low catalytic activity of CA enzymes in the tissues can cause many problems in metabolism. If metabolism cannot eliminate these problems, various disorders that cause edema, glaucoma, cancer, epilepsy, obesity, and osteoporosis occur. Therefore, using drugs with inhibitor/activator potential to keep this enzyme activity at an average level is one of the therapeutic targets [18–20].

Sulfonamides are widely used, such as brinzolamide, dorzolamide, methazolamide, acetazolamide, dichlorphenamide, and ethoxzolamide, in the treatment of many diseases as antitumor, antiglaucoma, antiobesity, anticonvulsant, and diuretic agents due to their remarkable inhibitory potential against CAs [20–22]. In literature, there are many primary and secondary sulfonamides and their derivatives can be found as potent and biologically active compounds targeting different types of diseases [20–25]. Among them, more specifically, secondary sulfonamides including sulfaguanidine and sulfisoxazole derivatives showed potential pharmaceutical activities [23–25]. In recent studies, multivalent inhibitors started to be investigated as potent and pharmaceutically active derivatives with ditopic interaction of the active site of enzyme(s) [23–26]. Taken together, in the present study, we used two well-known sulfa drugs (sulfisoxazole and sulfaguanidine) as pharmacophore groups and multivalent inhibitor design strategy was applied with bis-isocyanates in order to produce bis-ureido-substituted derivatives.

This study focused on the synthesis and inhibitory effects of bis-ureido-substituted sulfaguanidine (**SG1–4**) and sulfisoxazole (**SO1–4**) derivatives against human *h*CA I and II isoforms and AChE. In order to test synthesized derivatives' free radical scavenging potentials, the DPPH

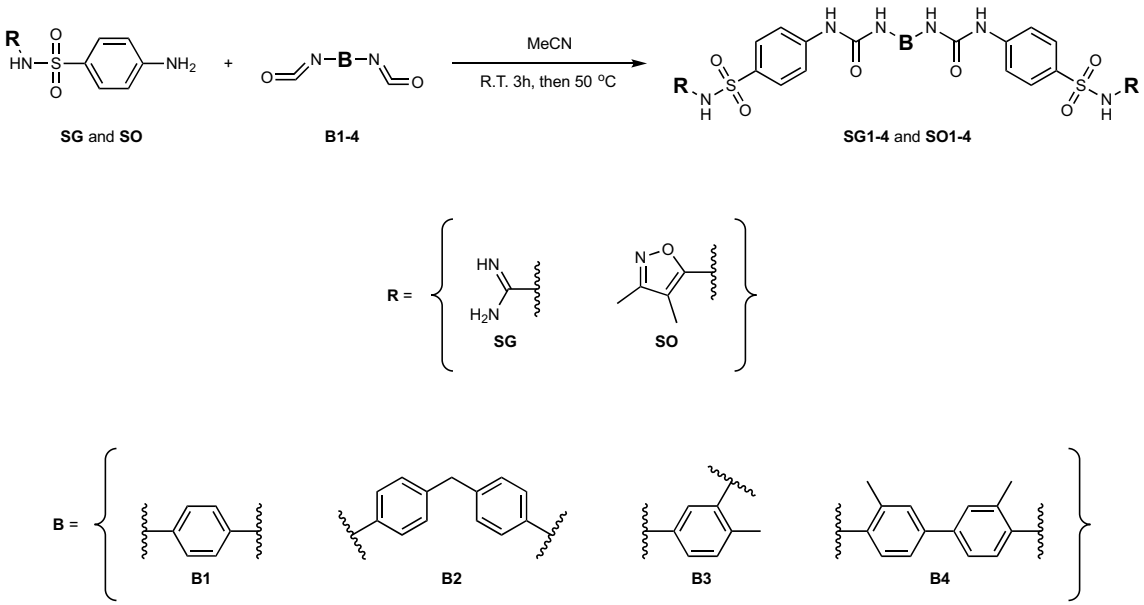

Scheme 1 General synthetic route for the synthesis of bis-ureido-substituted sulfisoxazole (**SG1–4**) and sulfaguanidine (**SO1–4**) derivatives

and ABTS assays methods were applied. In silico studies elucidated possible binding mechanisms of inhibitors to the active site.

Experimental

General procedure for the preparation of the compounds

Sulfaguanidine (**SG**)/Sulfisoxazole (**SO**) (2 mmol) was dissolved in acetonitrile (10–15 mL) and then treated with subsequent bis-isocyanates (1 mmol) (1,4-phenylene diisocyanide for **B1**, 4,4′-methylenebis(phenyl isocyanate) for **B2**, 4-methyl-1,3-phenylene diisocyanate for **B3**, 3,3'-dimethyl-4,4'-biphenylene diisocyanate for **B4**). The mixture was stirred at room temperature for 3 h, and then heated at 50 °C until completion (TLC monitoring). The obtained precipitate was filtered off, washed with diethyl ether (50 mL) and water, and dried in vacuo. The final pure products were characterized in detail by spectroscopic and analytic methods (FT-IR, ^{1}H-NMR, ^{13}C-NMR, and melting points) (Scheme 1).

4′-(((1,4-Phenylenebis(azanediyl))bis(carbonyl)) bis(azanediyl))bis(N-(3,4-dimethylisoxazol-5-yl) benzenesulfonamide) (SO1)

Yield: 72%; Color: white solid; Melting Point: 287–290 °C; Anal. Calcd for $C_{30}H_{30}N_8O_8S_2$ (694.74 g/mol) (%): C, 51.87; H, 4.35; N, 16.13; S, 9.23, Found (%): C, 51.81; H, 4.32; N, 16.18; S, 9.17; FT-IR (cm^{-1}): 3319, 3264 (NH), 1644 (C=O), 1550, 1339, 1157 (symmetric) (S=O), 1092; ^{1}H-NMR (DMSO-d_6, 500 MHz, δ ppm): 9.13 (s, 2H, –NH–CO–), 8.72 (s, 2H, –NH–CO–), 7.67–7.57 (m, 8H, Ar–H), 7.41–7.25 (m, 4H, Ar–H), 2.06 (s, 6H, –CH_3), 1.61 (s, 6H, –CH_3); ^{13}C-NMR (DMSO-d_6, 125 MHz, δ ppm): 162.01, 156.05, 152.72, 144.78, 134.32, 132.36, 128.44, 119.99, 118.16, 106.53, 10.70, 6.21.

4′-((((Methylenebis(4,1-phenylene)) bis(azanediyl))bis(carbonyl))bis(azanediyl)) bis(N-(3,4-dimethylisoxazol-5-yl) benzenesulfonamide) (SO2)

Yield: 66%; Color: white solid; Melting Point: 258–261 °C; Anal. Calcd for $C_{37}H_{36}N_8O_8S_2$ (778.82 g/mol) (%): C, 49.35; H, 4.40; N, 21.58; S, 8.23, Found (%): C, 49.30; H, 4.32; N, 21.65; S, 8.20; FT-IR (cm^{-1}): 3308, 3268 (NH), 1646 (C=O), 1540, 1339, 1157(symmetric) (S=O), 1092; ^{1}H-NMR (DMSO-d_6, 500 MHz, δ ppm): 9.13 (s, 2H, –NH–CO–), 8.73 (s, 2H, –NH–CO–), 7.66–7.57 (m, 8H, Ar–H), 7.34 (d, J = 8.0 Hz, 4H, Ar–H), 7.13 (d, J = 8.5 Hz, 4H, Ar–H), 3.80 (s, 2H, –CH_2–), 2.05 (s, 6H, –CH_3), 1.60 (s, 6H, –CH_3); ^{13}C-NMR (DMSO-d_6, 125 MHz, δ ppm): 162.01, 155.99, 152.65, 144.75, 137.31, 136.20, 132.36, 129.43, 128.44, 119.37, 118.99, 106.59, 40.25, 10.69, 6.21.

4′-((((4-Methyl-1,3-phenylene) bis(azanediyl))bis(carbonyl))bis(azanediyl)) bis(N-(3,4-dimethylisoxazol-5-yl) benzenesulfonamide) (SO3)

Yield: 63%; Color: white solid; Melting Point: 230–233 °C; Anal. Calcd for $C_{31}H_{32}N_8O_8S_2$ (708.77 g/mol) (%): C, 52.53; H, 4.55; N, 15.81; S, 9.05, Found (%): C, 52.46; H, 4.48; N, 15.88; S, 9.04; FT-IR (cm^{-1}): 3392, 3326 (NH), 1679 and 1652 (C=O), 1592, 1311, 1162 (symmetric) (S=O), 1095; ^{1}H-NMR (DMSO-d_6, 500 MHz, δ ppm): 9.52 (s, 1H, –NH–CO–), 9.07 (s, 1H, –NH–CO–), 8.78 (s, 1H, –NH–CO–), 8.06 (s, 1H, –NH–CO–), 7.94 (s, 1H, Ar–H), 7.69–7.58 (m, 6H, Ar–H), 7.15–7.07 (m, 4H, Ar–H), 2.17 (s, 3H, –CH_3), 2.06 (s, 3H, –CH_3), 2.06 (s, 3H, –CH_3), 1.61 (s, 3H, –CH_3), 1.60 (s, 3H, –CH_3); ^{13}C-NMR (DMSO-d_6, 125 MHz, δ ppm): 162.01, 156.00, 152.70, 152.55, 144.81, 144.75, 137.60, 137.36, 132.37, 132.33, 130.86, 128.54, 128.44, 122.56, 118.33, 118.01, 114.22, 112.37, 106.60, 17.93, 10.71, 6.22, 6.21.

4′-((((3,3′-Dimethyl-[1,1′-biphenyl]-4 ,4′-diyl)bis(azanediyl)) bis(carbonyl)) bis(azanediyl)) bis(N-(3,4-dimethylisoxazol-5-yl) benzenesulfonamide) (SO4)

Yield: 71%; Color: white solid; Melting Point: > 300 °C; Anal. Calcd for $C_{38}H_{38}N_8O_8S_2$ (798.89 g/mol) (%): C, 57.13; H, 4.79; N, 14.03; S, 8.03, Found (%): C, 57.07; H, 4.72; N, 14.12; S, 7.98; FT-IR (cm^{-1}): 3320, 3257 (NH), 1651 (C=O), 1590, 1340, 1158 (symmetric) (S=O), 1090; ^{1}H-NMR (DMSO-d_6, 500 MHz, δ ppm): 9.52 (s, 2H, –NH–CO–), 8.14 (s, 2H, –NH–CO–), 7.82 (d, J = 8.5 Hz, 3H, Ar–H), 7.66–7.61 (m, 7H, Ar–H), 7.49 (s, 2H, Ar–H), 7.44 (d, J = 8.5 Hz, 2H, Ar–H), 2.29 (s, 6H, –CH_3), 2.06 (s, 6H, –CH_3), 1.62 (s, 6H, –CH_3); ^{13}C-NMR (DMSO-d_6, 125 MHz, δ ppm): 162.02, 156.01, 152.81, 144.81, 136.26, 135.18, 132.36, 129.23, 128.53, 124.49, 122.40, 118.06, 106.60, 18.34, 10.70, 6.22.

4′-(((1,4-Phenylenebis(azaned iyl))bis(carbonyl))bis(azanediyl)) bis(N-carbamimidoylbenzenesulfonamide) (SG1)

Yield: 76%; Color: cream solid; Melting Point: > 300 °C; Anal. Calcd for $C_{22}H_{24}N_{10}O_6S_2$ (588.62 g/mol) (%): C, 44.89; H, 4.11; N, 23.80; S, 10.89, Found (%): C, 44.80; H, 4.05; N, 23.92; S, 10.82; FT-IR (cm^{-1}): 3443, 3337, 3219 (NH), 1674 (C=O), 1613, 1312, 1126 (symmetric) (S=O), 1093; ^{1}H-NMR (DMSO-d_6, 500 MHz, δ ppm): 8.93 (s, 2H, –NH–CO–), 8.64 (s, 2H, –NH–CO–), 7.64 (d, J = 9.0 Hz, 4H, Ar–H), 7.52 (d, J = 8.5 Hz, 4H, Ar–H), 7.38–7.32 (m, 4H, Ar–H), 6.64 (br.s, 8H, guanidine); ^{13}C-NMR (DMSO-d_6, 125 MHz, δ ppm): 158.42, 152.81, 142.83, 137.62, 134.40, 127.34, 119.76, 119.42, 117.74, 67.47.

4′-((((Methylenebis(4,1-phenylene)) bis(azanediyl))bis(carbonyl))bis(azanediyl)) bis(N-carbamimidoylbenzenesulfonamide) (SG2)

Yield: 68%; Color: white solid; Melting Point: 290–293 °C; Anal. Calcd for $C_{29}H_{30}N_{10}O_6S_2$ (678.74 g/mol) (%): C, 51.32; H, 4.46; N, 20.64; S, 9.45, Found (%): C, 51.23; H, 4.52; N, 20.69; S, 9.40; FT-IR (cm^{-1}): 3448, 3340, 3234 (NH), 1687 (C=O), 1641, 1309, 1134 (symmetric) (S=O), 1086; ^{1}H-NMR (DMSO-d_6, 500 MHz, δ ppm): 8.93 (s, 2H, –NH–CO–), 8.67 (s, 2H, –NH–CO–), 7.65 (d, J = 9.0 Hz, 4H, Ar–H), 7.52 (d, J = 9.0 Hz, 4H, Ar–H), 7.37–7.30 (m, 4H, Ar–H), 7.15–7.08 (m, 4H, Ar–H), 6.65 (br.s, 8H, guanidine), 3.81 (s, 2H, –CH_2–); ^{13}C-NMR (DMSO-d_6, 125 MHz, δ ppm): 158.42, 152.75, 142.77, 137.67, 135.88, 129.41, 128.14, 119.11, 117.76, 67.48, 25.56.

4′-((((4-Methyl-1,3-phenylene) bis(azanediyl))bis(carbonyl))bis(azanediyl)) bis(N-carbamimidoylbenzenesulfonamide) (SG3)

Yield: 62%; Color: white solid; Melting Point: 260–263 °C; Anal. Calcd for $C_{23}H_{26}N_{10}O_6S_2$ (602.65 g/mol) (%): C, 45.84; H, 4.35; N, 23.24; S, 10.64, Found (%): C, 45.73; H, 4.32; N, 23.29; S, 10.58; FT-IR (cm^{-1}): 3438, 3333, 3215 (NH), 1674 (C=O), 1618, 1311, 1127 (symmetric) (S=O), 1090; ^{1}H-NMR (DMSO-d_6, 500 MHz, δ ppm): 9.34 (s, 1H, –NH–CO–), 8.85 (s, 1H, –NH–CO–), 8.72 (s, 1H, –NH–CO–), 7.99 (s, 1H, –NH–CO–), 7.95 (s, 1H, Ar–H), 7.68–7.61 (m, 3H, Ar–H), 7.59–7.48 (m, 3H, Ar–H), 7.38 (d, J = 8.5 Hz, 2H, Ar–H), 7.16–7.05 (m, 2H, Ar–H), 2.18 (s, 3H, –CH_3); ^{13}C-NMR (DMSO-d_6, 125 MHz, δ ppm): 158.42, 158.37, 152.78, 152.66, 151.81, 142.84, 137.88, 137.68, 137.64, 131.14, 130.79, 127.70, 127.22, 127.14, 121.80, 117.73, 117.64, 113.65, 112.84, 111.79, 67.47, 17.64.

4′-((((3,3′-Dimethyl-[1,1′-biphenyl]-4,4′-diyl) bis(azanediyl))bis(carbonyl)) bis(azanediyl)) bis(N-carbamimidoylbenzenesulfonamide) (SG4)

Yield: 70%; Color: cream solid; Melting Point: > 300 °C; Anal. Calcd for $C_{30}H_{32}N_{10}O_6S_2$ (692.77 g/mol) (%): C, 52.01; H, 4.66; N, 20.22; S, 9.26, Found (%): C, 51.95; H, 4.60; N, 20.26; S, 9.21; FT-IR (cm^{-1}): 3441, 3333, 3221 (NH), 1691 (C=O), 1622, 1308, 1127 (symmetric) (S=O), 1090; ^{1}H-NMR (DMSO-d_6, 500 MHz, δ ppm): 9.35 (s, 2H, –NH–CO–), 8.07 (s, 2H, –NH–CO–), 7.88 (d, J = 8.5 Hz, 2H, Ar–H), 7.67 (d, J = 8.5 Hz, 4H, Ar–H), 7.56 (d, J = 9.0 Hz, 4H, Ar–H), 7.49 (s, 2H, Ar–H), 7.44

(d, $J = 8.5$ Hz, 2H, Ar–H), 6.66 (br.s, 8H, guanidine), 2.31 (s, 6H, $–CH_3$); ^{13}C-NMR (DMSO-d_6, 125 MHz, δ ppm): 158.44, 152.87, 142.84, 137.68, 136.56, 134.86, 128.68, 128.43, 127.70, 124.44, 123.94, 117.67, 112.84, 67.47, 18.43.

Biological studies

AChE and *h*CAs activity assay

First, the purification of CA isoenzymes (*h*CA I and *h*CA II) from human erythrocytes was performed according to the modified procedure described in the literature [27, 28]. In the inhibition studies, according to our previous studies [29–31], the esterase activities of *h*CA isoforms were determined by the *p*-nitrophenylacetate that used as a substrate converted by both isoforms to the p-nitrophenolate ion in this technique [32, 33]. The AChE activity was performed by a modified version of the Ellman method [34, 35], and inhibitory effect of the novel bis-ureido-substituted sulfaguanidine (**SG1–4**) and sulfisoxazole (**SO1–4**) derivatives was examined using acetylthiocholine iodide (ATChI) as the substrates and 5,5-Dithiobis(2-nitrobenzoic) acid (DTNB). The activity results were monitored spectrophotometrically at 412 nm [36, 37].

*h*CAs and AChE kinetic assay

The inhibition effects of the novel bis-ureido-substituted sulfaguanidine (**SG1–4**) and sulfisoxazole (**SO1–4**) derivatives were determined with at least five different inhibitor concentrations on against *h*CAs and AChE. The IC_{50}s of the synthesized derivatives (**SG1–4** and **SO1–4**) was calculated from Activity (%) − [Derivative] graphs for each derivatives according to our previous studies [38–41]. The inhibition types and K_Is values were found by Lineweaver and Burk's curves [41–44] (Table 1).

Free radical scavenging effect studies

DPPH scavenging activity of synthesized derivatives and standard antioxidants was performed by the Blois method [45]. 0.1 mM DPPH$^{\bullet}$ solution was prepared in methanol, and 1 mL of this solution was taken from 10, 20, 40 mL of stock solutions at different concentrations to make up 3 mL of ethanol and added to the sample solution. 0.1 mM solution of DPPH in methanol was prepared and 1 mL of this solution was made up to a final volume of 3 mL. The solutions were vortexed and then incubated in the dark for 30 min, and their absorbance was measured at 517 nm (Table 2).

It was made by the color change method, which indicates that the dark blue/green colored ABTS$^{\bullet+}$ radical has lost its radical characteristic as a result of chemical reaction with antioxidants [46]. The ABTS$^{\bullet+}$ radical was obtained by mixing the ABTS solution prepared with 2 mmol L^{-1} H_2O and 2.45 mmol L^{-1} of potassium persulfate ($K_2S_20_8$) solution at a ratio of 1:2 and incubating for 14 h in the dark and at room temperature. Before using the ABTS$^{\bullet+}$ radical, the solution was diluted with sodium phosphate buffer (0.1 mol L^{-1}, pH 7.4) to obtain an absorbance of 0.750 ± 0.025. Then 10, 20, 40 µL of the stock solutions of the synthesized derivatives were added to the phosphate buffer until its volume became 3 mL, then 1 mL of ABTS$^{\bullet+}$ solution was added and vortexed. These solutions were incubated in the dark for 30 min, and their absorbance was measured at 734 nm.

Molecular docking studies

The in silico molecular docking analysis and design of correlation figures were performed within the Schrödinger Small-Molecule Drug Discovery Suite 2021-2 for Mac (Schrödinger, LLC, NY, USA) using the panels: Maestro version 12.8, LigPrep [47], Protein Preparation Wizard [48], Receptor Grid Generation [49], Ligand Docking, and Prime MM-GBSA. Initially, the crystal structures of *h*CA I (PDB: 6F3B, species Homo sapiens) [50], *h*CA II (PDB: 6H34, species Homo sapiens) [51], and AChE (PDB: 4BDT, species Homo sapiens) [52] were downloaded from the Protein Data Bank (https://www.rcsb.org) [53], prepared and optimized using the Maestro [54]. The novel bis-ureido-substituted sulfaguanidine (**SG1–4**) and sulfisoxazole (**SO1–4**) derivatives were built by the ChemDraw version 20 for Mac (PerkinElmer, Inc., Waltham, MA, USA) [55] and suitably optimized for docking by the LigPrep tool [56]. Epik [57] with default conditions was used in the OPLS4 force field at pH 7.0 ± 2.0 [58]. The grid boxes for 6F3B, 6H34, and 4BDT were created using the Receptor Grid Generation tool [59], and the Glide extra precision (XP) [60–63] option of the Ligand Docking tool was utilized to dock the bis-ureido-substituted sulfaguanidine and sulfisoxazole inhibitors (**SG1–4** and **SO1–4**) in the binding site of the enzymes. The docking scores were used to score the poses of these compounds (**SG1–4** and **SO1–4**) and to evaluate their binding affinity versus the binding site of 6F3B, 6H34, and 4BDT. MM-GBSA solvation in the VSGB energy model [64–66] and OPLS4 force field was used to compute the binding energies for the best poses of *h*CA I, *h*CA II, and AChE with the novel bis-ureido-substituted derivatives (**SG1–4** and **SO1–4**) derived from Glide XP docking [67–70].

Statistical studies

Analysis of the data and drawing of graphs were realized using GraphPad Prism version 8 for Mac (GraphPad Software, La Jolla California USA). The inhibition constants

Table 1 Inhibition data of bis-ureido-substituted sulfaguanidine (**SG1–4**) and sulfisoxazole (**SO1–4**) derivatives against *h*CA I, *h*CA II, and AChE

ID	*h*CA I			*h*CA II			AChE			Selectivity Index[b]	
	K_I (nM)[a]	R^2	Inhibition type	K_I (nM)[a]	R^2	Inhibition type	K_I (nM)[a]	R^2	Inhibition type	*h*CA I/*h*CA II	*h*CA II/*h*CA I
SG1	41.02 ± 7.52	0.9479	Competitive	41.42 ± 7.51	0.9546	Competitive	344.80 ± 57.11	0.9607	Competitive	0.99	1.01
SG2	28.72 ± 6.11	0.9451	Competitive	13.86 ± 2.53	0.9557	Competitive	285.40 ± 55.94	0.9470	Competitive	2.07	0.48
SG3	27.34 ± 5.54	0.9480	Competitive	67.14 ± 13.58	0.8688	Noncompetitive	442.60 ± 52.13	0.9770	Competitive	0.41	2.46
SG4	2.54 ± 0.50	0.9512	Competitive	27.12 ± 3.86	0.9440	Noncompetitive	315.30 ± 55.29	0.9571	Competitive	0.09	10.68
SO1	16.97 ± 5.27	0.8484	Competitive	25.65 ± 7.11	0.9023	Competitive	314.30 ± 62.65	0.9416	Competitive	0.66	1.51
SO2	13.40 ± 2.03	0.9678	Competitive	11.92 ± 1.82	0.9688	Competitive	425.70 ± 46.30	0.9468	Noncompetitive	1.12	0.89
SO3	17.56 ± 11.30	0.8840	Competitive	35.79 ± 4.79	0.9251	Noncompetitive	286.00 ± 45.62	0.9620	Competitive	0.49	2.04
SO4	3.38 ± 0.57	0.9609	Competitive	11.20 ± 2.97	0.9041	Competitive	257.60 ± 27.84	0.9827	Competitive	0.30	3.31
AAZ [c]	439.17 ± 9.30	0.9990	Noncompetitive	98.28 ± 1.69	0.9992	Noncompetitive	–	–	–	–	–
THA [d]	–	–	–	–	–	–	155.29 ± 0.82	0.9999	Competitive	–	–

[a]The test results were expressed as means of triplicate assays ± SEM

[b]The K_I rates are indicative of selectivity index: A potent selective inhibitor is characterized by a high-value ratio

[c]Acetazolamide

[d]Tacrine

Table 2 The radical scavenging activity of bis-ureido-substituted sulfaguanidine (**SG1–4**) and sulfisoxazole (**SO1–4**) derivatives

ID	DPPH[a,b] (0.2 mg/mL)	ABTS[a,b] (0.2 mg/mL)
SG1	10.31 ± 0.40	69.71 ± 4.63
SG2	7.35 ± 0.39	12.90 ± 0.96
SG3	8.11 ± 0.54	21.14 ± 3.27
SG4	9.57 ± 0.70	27.36 ± 1.41
SO1	18.20 ± 1.53	78.85 ± 6.25
SO2	7.40 ± 0.36	31.85 ± 2.24
SO3	14.19 ± 0.99	28.53 ± 3.73
SO4	8.46 ± 0.60	41.65 ± 5.63
Trolox[c]	70.10 ± 6.63	90.36 ± 6.95

[a]The test results were expressed as means of triplicate assays ± SEM

[b]Values are expressed as percent radical scavenging activity

[c]Standard antioxidants

were calculated by SigmaPlot version 12 for Windows (Systat Software, San Jose California USA). The fit of enzyme inhibition models was compared using the extra sum-of-squares F test and the AICc approach. The results were exhibited as mean ± standard error of the mean (95% confidence intervals). Differences between datasets were considered statistically significant when the *p*-value was less than 0.05.

Results and discussion

Drug design strategy and chemistry

Ureido-substituted compounds were started to be investigated as a potent and selective carbonic anhydrase inhibitor, and among them, one of the compounds (**SLC-0111**) reached phase II clinical trials to treat advanced metastatic solid tumors [71–73]. On the other hand, compounds that contain bis-aromatic and heterocyclic moieties showed excellent inhibition/activation properties due to their ditopic interactions on the active site of the enzyme(s) [23–25]. In the present study, we wanted to use the potency of ureido-substituted compounds and improve their activity with bis-substitution. For these reasons, sulfaguanidine and sulfisoxazole were used as starting materials (as a pharmacophore group since they have strong binding efficiency to the active site of the enzymes that were used in the present study), and bis-ureido substitution was applied to make new compounds. The chemical diversity was obtained by using different aromatic bis-isocyanates such as 1,4-phenylene diisocyanide for **B1**, 4,4′-methylenebis(phenyl isocyanate) for **B2**, 4-methyl-1,3-phenylene diisocyanate for **B3**, and 3,3'-dimethyl-4,4'-biphenylene diisocyanate for **B4**. The synthesis of a series of bis-ureido-substituted compounds was performed according to the general synthetic route as demonstrated in Scheme 1. Briefly, the sulfaguanidines and sulfisoxazoles were conjugated with bis-isocyanates to produce bis-ureido-substituted compounds **SG1–4** and **SO1–4** using acetonitrile as a solvent and under mild conditions (R.T. to 50 °C).

By adding different functional groups to the compounds, versatile bioactive properties can be gained, thus, increasing the importance of those compounds. For example, potent cholinesterase and CA inhibitors used in the treatment of many diseases are being developed by synthesizing analogues of standard compounds such as sulfonamides with high efficacy [74]. In this way, sulfa drugs are designed to treat many different diseases [37, 75, 76]. Studies have focused on the synthesis and design of sulfa derivatives, versatile agents that will be alternatives to inhibitors with therapeutic effects. In this study, the inhibition effects of novel bis-ureido-substituted sulfaguanidine (**SG1–4**) and sulfisoxazole (**SO1–4**) derivatives on *h*CAs and AChE were investigated as in vitro and in silico studies.

Biological studies

*h*CAs and AChE inhibition study and structure–activity relationship assay

CAs are metalloenzymes that act as catalysts for the reversible hydration of CO_2 to bicarbonate and protons in all living organisms. However, because they are also metabolic enzymes, this superfamily of enzymes plays a significant role in physiologic processes [77–79]. Here, the activity of the newly synthesized bis-ureido-substituted compounds against two physiologically and pharmacologically important isoforms, cytosolic isoforms *h*CA I and II, was tested. Table 1 displays that both sulfaguanidine (**SG1–4**) and sulfisoxazole (**SO1–4**) derivatives in novel bis-ureido-substituted series are more active inhibitors of the *h*CA I isoform when compared to *h*CA II. The novel synthesized compounds **SG1–4** and **SO1–4** exhibited low nanomolar range inhibition against *h*CA I than standard drug acetazolamide (AAZ, $K_I = 439.17 \pm 9.30$ nM). Compound **SG4** (Fig. 1) in sulfaguanidines (**SG1–4**) and compound **SO4** in sulfisoxazoles (**SO1–4**), containing 3,3′-dimethyl-4,4′-biphenylene diisocyanate moiety (**B4**), displayed a K_I values of 2.54 ± 0.50 and 3.38 ± 0.57 nM, respectively, against *h*CA I. The relocation of moiety **B4** with 1,4-phenylene diisocyanide (**B1**) and 4-methyl-1,3-phenylene diisocyanate (**B3**) did not increase inhibitory actions versus *h*CA I for compounds **SG1** and **SO3** and even decreased in activity was observed compared to compounds **SG4** and **SO4**, 16 and fivefold, respectively. However, significantly, compounds **SO1** and **SO2**, possessing **B1** ($K_I = 16.97 \pm 5.27$ nM) and 4,4′-methylenebis(phenyl

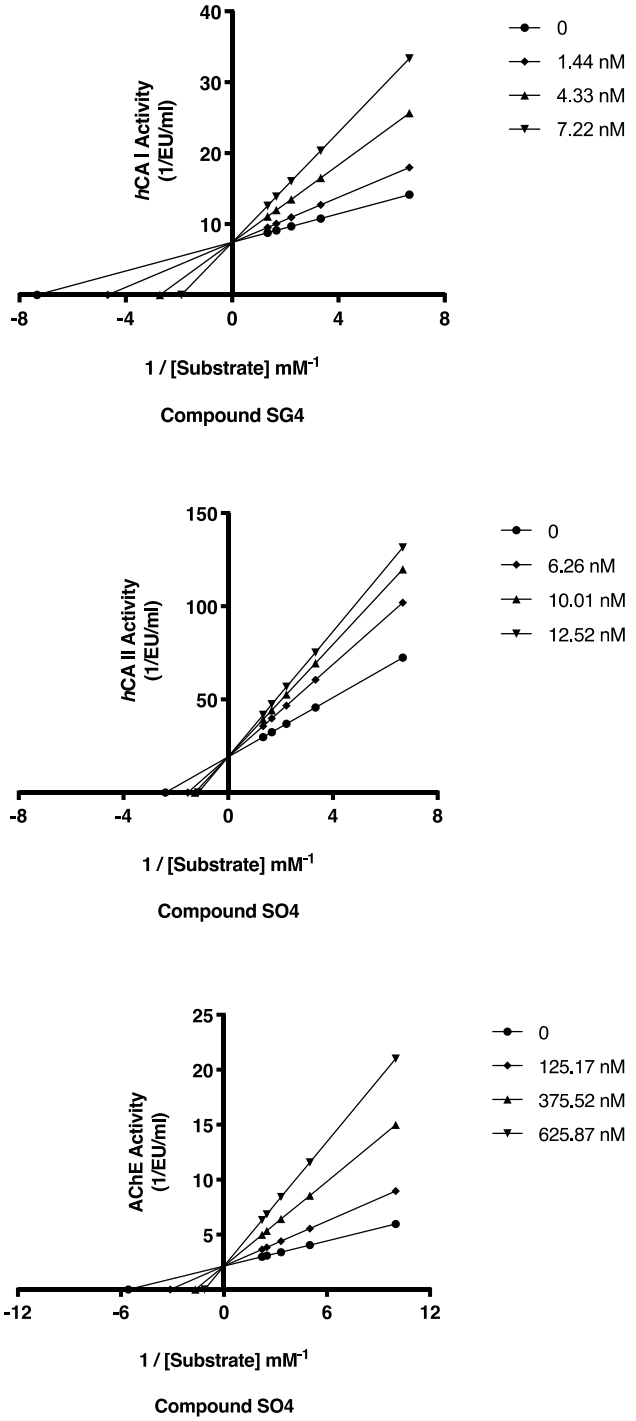

Fig. 1 Lineweaver–Burk curves used to determine the K_I constants and inhibition types of the most potent inhibitors, **SG4** (for *h*CA I) and **SO4** (for *h*CA II and AChE)

isocyanate) (**B2**) ($K_I = 13.40 \pm 2.03$ nM) substituents, respectively, displayed weaker inhibitory action than compound **SO4**. Of note, the compounds having sulfaguanidine group (**SG1-4**) did not exhibit more effective inhibition compared to the sulfisoxazoles (**SO1-4**) against *h*CA I, showing K_Is in the range of 27.34 ± 5.54 to 28.72 ± 6.11 nM, which shows the sulfisoxazole is much better pharmacophore than sulfaguanidine targeting *h*CA I isoform. As a result of these initial results, new, biologically potent and *h*CA I selective compounds might be obtained by using sulfisoxazole as a pharmacophore group and bis-substitution technique.

*h*CA II was effectively inhibited by these derivatives (**SG1–4** and **SO1–4**), and all of the compounds were low nanomolar inhibitors than the standard drug AAZ ($K_I = 98.28 \pm 1.69$ nM) (Table 1). Compound **SO4** ($K_I = 11.20 \pm 2.97$ nM) bearing **B4** moiety showed low nanomolar inhibition against *h*CA II (Fig. 1). Noticeably, **B2** substituted derivative **SO2** was a promising inhibitor for *h*CA II and showed a K_I value of 11.92 ± 1.82 nM. In contrast, **B1**-substituted compound **SG1** and **B3**-substituted compound **SG3** (K_Is $= 41.42 \pm 7.51$ and 67.14 ± 13.58 nM, respectively) were the least effective *h*CA II inhibitors among all compounds (**SG1–4** and **SO1–4**). The order of inhibitory activities for the bis-ureido-substituted sulfaguanidine (**SG1-4**) and sulfisoxazole (**SO1–4**) derivatives against *h*CA II were in the order of **SO4** > **SO2** > **SG2** > **SO1** > **SG 4** > **SO3** > **SG1** > **SG3**. These results show that bis-phenyl linker in between the pharmacophore groups can improve the potency and selectivity of compounds against *h*CA II isozyme.

According to the off-target/target *h*CA selectivity ratio summarized in Table 1, most of the synthesized compounds showed interesting degrees of selectivity against the isoform *h*CA I over *h*CA II. Particularly, derivatives **SG4** and **SO4** having **B4** moiety showed the most pronounced selectivity against *h*CA I over the *h*CA II isoform, with selectivity index (*SI*; *h*CA I/*h*CA II) values of 0.09 and 0.30, respectively, i.e., *SI* (*h*CA II/*h*CA I) = 10.68 and 3.31, respectively. The compounds (**SG2** and **SO2**) bearing the **B2** group of the **SG1–4** and **SO1–4** series displayed selectivity against *h*CA II over *h*CA I isoform, with *SI* (*h*CA II/*h*CA I) values of 0.48 and 0.89, respectively, i.e., *SI* (*h*CA I/*h*CA II) = 2.07 and 1.12, respectively.

AChEIs are the first generation of medications used to treat AD, glaucoma, myasthenia gravis, and a variety of other neuromuscular illnesses. It has a restriction in that as the level of ACh rises, the symptoms of these disorders rise as well. Thus, the search for novel AChEIs is highly valued for further improvement in the treatment of such disorders [80, 81]. Thus, finally, inhibition of the AChE proceeded at the highest concentrations of the tested enzymes. AChE was inhibited by both sulfaguanidine (**SG1–4**) and sulfisoxazole (**SO1–4**) derivatives at nanomolar concentrations (K_I values of 257.60 ± 27.84–442.60 ± 52.13 mM). By varying the nature of the substitute in the bis-ureido group, it was determined that the most potent inhibitor of the AChE was the **B4** analogue, **SO4** ($K_I = 257.60 \pm 27.84$ nM) (Fig. 1) compared with other

derivatives but close to the value of **B2** compound **SG2** ($K_I = 285.40 \pm 55.94$ nM). However, the AChE inhibitory activities for the bis-ureido-substituted sulfaguanidine (**SG1–4**) and sulfisoxazole (**SO1–4**) derivatives reduced in the order of **SO4** > **SG2** > **SO3** > **SO1** > **SG4** > **SG1** > **SO2** > **SG3**. Moreover, a **B4** compound **SO4** showed a parallel tendency, i.e., it was the most active inhibitor against both *h*CA II and AChE. Interestingly, the last observations are consistent with the data for the *h*CA I, II isoforms, and AChE.

Recently, an increasing number of different *h*CAIs and AChEIs than the sulfonamides and their bioisosteres have been identified. In this context, the study by Tugrak et al. [82] reported that new series of imidazolinone-based benzenesulfonamides were synthesized, and some of them were in the structure of sulfaguanidine (**3b** and **4b**). They analyzed the compounds against *h*CA I, II, and AChE enzymes to discover possible novel drug candidates and determined that tested sulfaguanidine derivatives, **3b** ($K_I = 16.89$ nM), and **4b** ($K_I = 14.81$ nM), were more potent inhibitors than the reference drug THA ($K_I = 18.45$ nM) while weak inhibitor against *h*CAs. Alyar et al. [83] reported that new Schiff bases **Ll**, **L2**, and **L3** derived from sulfamethoxazole (**S1**)/ sulfisoxazole (**S2**) and substituted salicylaldehydes and their Pd(II), Cu(II) complexes were synthesized for the first time. The inhibition activities of these compounds on *h*CAs have been investigated and found that have high inhibition potencies on enzymes. Mert et al. [84] synthesized a series of sulfadiazine and sulfisoxazole derivatives starting from 1-(3-nitrophenyl)-5-phenyl-1*H*-pyrazole-3,4-dicarboxylic acid. They characterized the structures of synthesized molecules by various spectroscopic methods and purified *h*CA I and II isoenzymes by the Sepharose-4B-L-tyrosine-sulfanilamide affinity column chromatography. They determined that compound **4** from the newly synthesized molecules possesses remarkable inhibition effects on *h*CA I.

Free radical scavenging effect assays

The amount of electron donation or the number and position of hydroxyl groups (-OH) in a compound's structure determines its free radical scavenging ability. One of the methods used to test the free radical scavenging capacity of antioxidants is the DPPH and ABTS assay, which is frequently used in research [85, 86]. The novel bis-ureido-substituted sulfaguanidine (**SG1–4**) and sulfisoxazole (**SO1–4**) derivatives demonstrated free radical scavenging capabilities in this study. The derivatives' ABTS radical scavenging potential (in the range of 12.9–78.8%) is often higher than that of DPPH (in the range of 7.3–10.3%). When the data are analyzed, the derivatives appear to be successful at eliminating free radicals that cause cellular damage.

Molecular docking study

To better understand the interaction of the novel bis-ureido-substituted sulfaguanidine (**SG1–4**) and sulfisoxazole (**SO1–4**) derivatives with 6F3B, 6H34, and 4BDT, the most potent *h*CA I, *h*CA II, and AChE inhibitors **SG4** (for *h*CA I) and **SO4** (for *h*CA II and AChE) were docked in the binding sites of these proteins. For the redocking computes, the structures of crystal ligands, including CJK (1-[(4-methylphenyl)methyl]-3-(2-oxidanyl-5-sulfamoyl-phenyl)urea, PubChem Ref.: 134817796), FKK (4-[4-[(4-fluorophenyl)methyl]piperazin-1-yl]carbonylbenzenesulfonamide, PubChem Ref.: 132844), and HUW (Huprine W, PubChem Ref.: 71463576) in the active sites were used (Fig. 2). The docked pose of HUW overlapped with the poses in the X-ray crystal structure (PDB: 4BDT) at a root mean square deviation (RMSD) value of 0.77 Å, whereas the docked poses of CJK and FKK X-ray structures (PDBs: 6F3B and 6H34) displayed RMSD values of 1.83 Å and 1.31 Å, respectively. After that, in the present docking study, the docking patterns of CJK, FKK, and HUW were compared with that of derivative **SG4** for *h*CA I (K_I: 2.54 ± 0.50 nM) and derivative **SO4** for *h*CA II and AChE (K_Is: 11.20 ± 2.97 nM and 257.60 ± 27.84 nM, respectively), the most potent compounds in this series (**SG1–4** and **SO1–4**). The binding interactions of the inhibitors with *h*CA I, *h*CA II, and AChE are displayed in Fig. 3.

Derivative **SG4** (Docking score value of − 1.594 kcal/mol and MM-GBSA value of 4.46 kcal/mol) formed H-bond with Asp4 (distance 1.84 Å), Thr199 (distance 2.19 Å), Pro201 (distance 1.96 Å), Val233 (distance 2.36 Å), and Asp236 (distance 2.41 Å), respectively, while benzene ring displayed π–π interaction with Trp5. Furthermore, compound **SG4** displayed that residues Tyr20, His64, His67, Phe91, Gln92, His94, His96, His119, Leu141, Val143, Lys170, Ser197, Leu198, His200, Pro202, Leu203, Val207, Trp209, and Asn232 play significant roles in the binding of the ligand with *h*CA I. The docking showed that derivative **SO4** (Docking score value of − 2.366 kcal/mol and MM-GBSA value of − 5.27 kcal/mol) formed three H-bonds with residues His64 (distance 2.68 Å) and Gln92 (distances 2.38 and 2.79 Å) of *h*CA II. Also, it displayed π − π and π − cation interactions with His3. Nevertheless, hydrophobic interactions were monitored between derivative **SO4** and residues Trp5, Ala65, Val121, Leu141, Val143, Leu198, Pro201, Pro202, Val207, and Trp209. Compound **SO4** (Docking score value of 2.753 kcal/mol and MM-GBSA value of − 29.33 kcal/mol) has an H-bond with Tyr337 (distance 1.84 Å). It also acted π − π interactions with Trp86 and Tyr337 from the binding site residues of AChE. Moreover, the derivative **SO4** interacted with some hydrophobic fragments, namely, Tyr72, Tyr124, Val282, Trp286, Val294, Phe295, Phe297, Phe338, Tyr341, Trp439, and Tyr449.

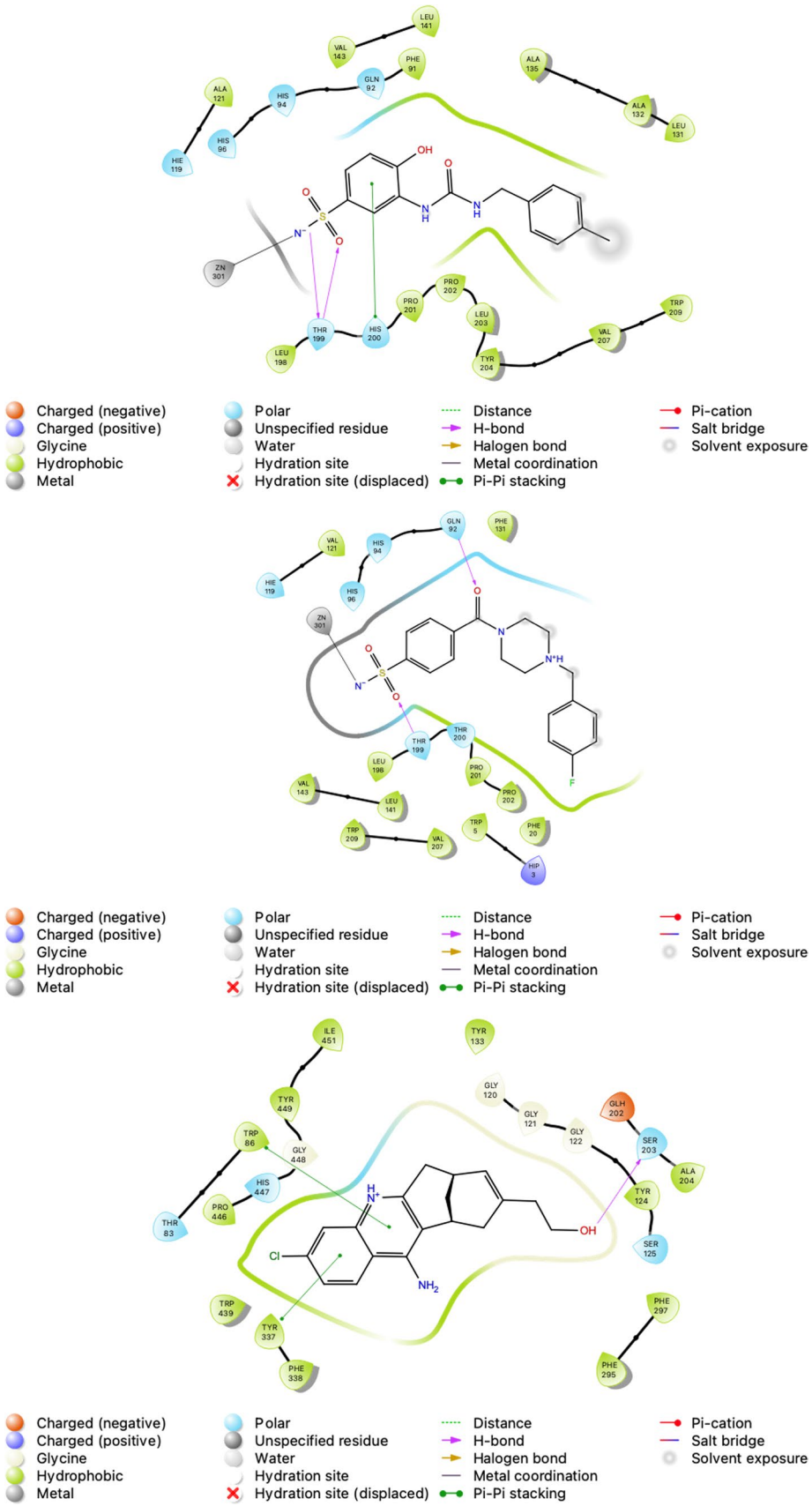

Fig. 2 The binding sites of *h*CA I (PDB: 6F3B) (top), *h*CA II (PDB: 6H34) (middle), and AChE (PDB: 4BDT) (bottom) with the docked poses of the native ligands CJK ($C_{15}H_{17}N_3O_4S$: 1-[(4-methylphenyl)methyl]-3-(2-oxidanyl-5-sulfamoyl-phenyl)urea, PubChem Ref.: 134817796), FKK ($C_{18}H_{20}FN_3O_3S$: 4-[4-[(4-fluorophenyl)methyl] piperazin-1-yl]carbonylbenzenesulfonamide, PubChem Ref.: 132844), and HUW ($C_{18}H_{19}ClN_2O$: Huprine W, PubChem Ref.: 71463576), respectively

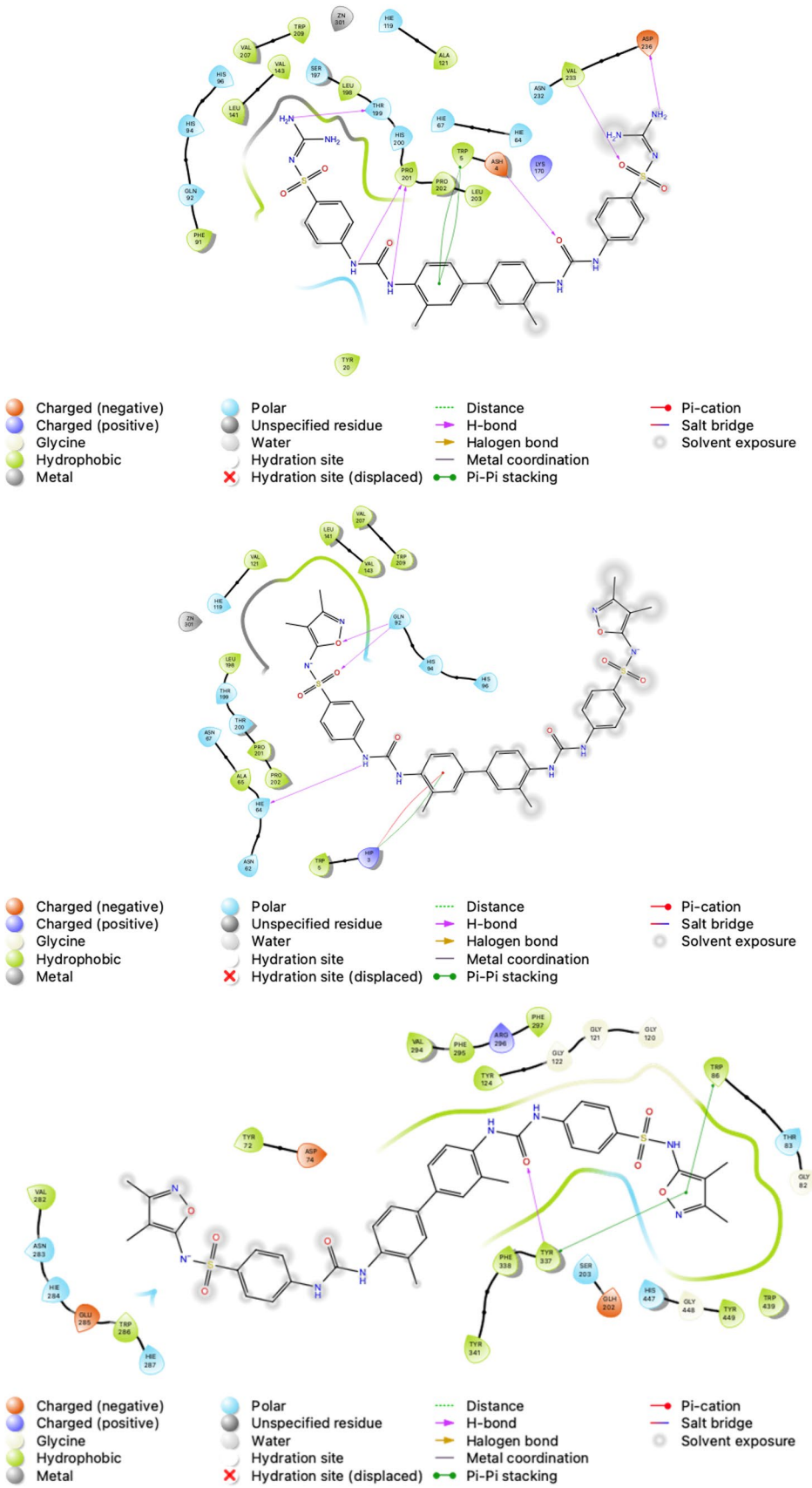

Fig. 3 The 2D binding modes of novel bis-ureido-substituted sulfaguanidine (**SG4**) and sulfisoxazole (**SO4**) derivatives in the binding sites of *h*CA I (6F3B with compound **SG4**) (top), *h*CA II (6H34 with compound **SO4**) (middle), and AChE (4BDT with compound **SO4**) (bottom)

Conclusion

A series of novel bis-ureido-substituted sulfaguanidine (**SG1–4**) and sulfisoxazole (**SO1–4**) derivatives were more effective than standard compounds used as selective *h*CA I and II inhibitors. As a result, the study may provide promising information to the literature for the synthesis of alternative molecules to the inhibitory drugs used for the treatment of diseases due to their effect on the removal of free radicals that cause cellular damage and their inhibitory capacity on metabolic enzymes (*h*CAs and AChE). In future studies, more effective drugs can be obtained by adding different groups to the derivatives of sulfo compounds and some of the studies under investigation in our laboratories. Furthermore, the bis-substituted compounds may get more attention due to their ditopic interactions on the targeted enzyme(s).

Supplementary Information The online version contains supplementary material available at https://doi.org/10.1007/s11030-022-10527-0.

Acknowledgements This work was supported by the Research Fund of Anadolu University (Grant Number 2102S003).

Declarations

Conflict of interest The authors declare that there is no conflict of interest.

References

1. Ferreira A, Proença C, Serralheiro M, Araujo M (2006) The in vitro screening for acetylcholinesterase inhibition and antioxidant activity of medicinal plants from Portugal. J Ethnopharmacol 108(1):31–37. https://doi.org/10.1016/j.jep.2006.04.010
2. Heinrich M, Teoh HL (2004) Galanthamine from snowdrop—the development of a modern drug against Alzheimer's disease from local Caucasian knowledge. J Ethnopharmacol 92(2–3):147–162. https://doi.org/10.1016/j.jep.2004.02.012
3. Işık M, Beydemir Ş (2019) AChE mRNA expression as a possible novel biomarker for the diagnosis of coronary artery disease and Alzheimer's disease, and its association with oxidative stress. Arch Physiol Biochem. https://doi.org/10.1080/13813455.2019.1683584
4. Voet D, Voet J, John W, Jhon S (1995) Serine proteases. Biochemistry 390:1–7
5. Tavares L, Fortalezas S, Tyagi M, Barata D, Serra AT, Martins Duarte CM et al (2012) Bioactive compounds from endemic plants of Southwest Portugal: Inhibition of acetylcholinesterase and radical scavenging activities. Pharm Biol 50(2):239–246. https://doi.org/10.3109/13880209.2011.596209
6. Knapp MJ, Knopman DS, Solomon PR, Pendlebury WW, Davis CS, Gracon SI et al (1994) A 30-week randomized controlled trial of high-dose tacrine in patients with Alzheimer's disease. JAMA 271(13):985–991
7. Haass C, Selkoe DJ (2007) Soluble protein oligomers in neurodegeneration: lessons from the Alzheimer's amyloid β-peptide. Nat Rev Mol Cell Biol 8(2):101–112. https://doi.org/10.1038/nrm2101
8. Stuchbury G, Münch G (2005) Alzheimer's associated inflammation, potential drug targets and future therapies. J Neural Transm 112(3):429–453. https://doi.org/10.1007/s00702-004-0188-x
9. Işık M (2019) The binding mechanisms and inhibitory effect of intravenous anesthetics on AChE in vitro and in vivo: kinetic analysis and molecular docking. Neurochem Res 44(9):2147–2155. https://doi.org/10.1007/s11064-019-02852-y
10. Calabrese V, Scapagnini G, Colombrita C, Ravagna A, Pennisi G, Stella AG et al (2003) Redox regulation of heat shock protein expression in aging and neurodegenerative disorders associated with oxidative stress: a nutritional approach. Amino Acids 25(3–4):437–444. https://doi.org/10.1007/s00726-003-0048-2
11. Gibson GE, Huang H-M (2005) Oxidative stress in Alzheimer's disease. Neurobiol Aging 5(26):575–578. https://doi.org/10.1016/j.neurobiolaging.2004.07.017
12. Işık M, Beydemir Ş, Yılmaz A, Naldan ME, Aslan HE, Gülçin İ (2017) Oxidative stress and mRNA expression of acetylcholinesterase in the leukocytes of ischemic patients. Biomed Pharmacotherapy. https://doi.org/10.1016/j.biopha.2017.01.003
13. Işık M, Demir Y, Kırıcı M, Demir R, Şimşek F, Beydemir Ş (2015) Changes in the anti-oxidant system in adult epilepsy patients receiving anti-epileptic drugs. Arch Physiol Biochem 121(3):97–102. https://doi.org/10.3109/13813455.2015.1026912
14. Mossa A, Nawwar G (2011) Free radical scavenging and antiacetylcholinesterase activities of *Origanum majorana* L. essential oil. Hum Experimental Toxicol 30(10):1501–1513. https://doi.org/10.1177/0960327110391686
15. Halliwell B, Gutteridge JM (2015) Free radicals in biology and medicine. Oxford University Press, Oxford
16. Tohma H, Isik M, Korkmaz M, Bursal E, Gulcin I, Koksal E (2015) Determination of antioxidant properties of Gypsophila bitlisensis bark. Int J Pharmacol 100(4):366–437. https://doi.org/10.3923/ijp.2015.366.371
17. Supuran CT (2008) Carbonic anhydrases: novel therapeutic applications for inhibitors and activators. Nat Rev Drug Discov 7(2):168–181. https://doi.org/10.1038/nrd2467
18. Capasso C, Supuran CT (2015) Bacterial, fungal and protozoan carbonic anhydrases as drug targets. Expert Opin Ther Targets 19(12):1689–1704. https://doi.org/10.1517/14728222.2015.1067685
19. Sarikaya SBÖ, Topal F, Şentürk M, Gülçin I, Supuran CT (2011) In vitro inhibition of α-carbonic anhydrase isozymes by some phenolic compounds. Bioorg Med Chem Lett 21(14):4259–4262. https://doi.org/10.1016/j.bmcl.2011.05.071
20. Alterio V, Di Fiore A, D'Ambrosio K, Supuran CT, De Simone G (2012) Multiple binding modes of inhibitors to carbonic anhydrases: how to design specific drugs targeting 15 different isoforms? Chem Rev 112(8):4421–4468. https://doi.org/10.1021/cr200176r
21. Carta F, Scozzafava A, Supuran CT (2012) Sulfonamides: a patent review (2008–2012). Expert Opin Ther Pat 22(7):747–758. https://doi.org/10.1517/13543776.2012.698264
22. Carta F, Vullo D, Osman SM, AlOthman Z, Supuran CT (2017) Synthesis and carbonic anhydrase inhibition of a series of SLC-0111 analogs. Bioorg Med Chem 25(9):2569–2576. https://doi.org/10.1016/j.bmc.2017.03.027
23. Akocak S, Alam MR, Shabana AM, Sanku RKK, Vullo D, Thompson H et al (2016) PEGylated bis-sulfonamide carbonic anhydrase inhibitors can efficiently control the growth of several carbonic anhydrase IX-expressing carcinomas. J Med Chem 59(10):5077–5088. https://doi.org/10.1021/acs.jmedchem.6b00492
24. Akocak S, Lolak N, Nocentini A, Karakoc G, Tufan A, Supuran CT (2017) Synthesis and biological evaluation of novel aromatic

and heterocyclic bis-sulfonamide Schiff bases as carbonic anhydrase I, II, VII and IX inhibitors. Bioorg Med Chem 25(12):3093–3097. https://doi.org/10.1016/j.bmc.2017.03.063
25. Akocak S, Lolak N, Bua S, Nocentini A, Supuran CT (2019) Activation of human α-carbonic anhydrase isoforms I, II, IV and VII with bis-histamine schiff bases and bis-spinaceamine substituted derivatives. J Enzyme Inhib Med Chem 34(1):1193–1198. https://doi.org/10.1080/14756366.2019.1630616
26. Yapar G, Duran HE, Lolak N, Akocak S, Türkeş C, Durgun M et al (2021) Biological effects of bis-hydrazone compounds bearing isovanillin moiety on the aldose reductase. Bioorg Chem. https://doi.org/10.1016/j.bioorg.2021.105473
27. Kalaycı M, Türkeş C, Arslan M, Demir Y, Beydemir Ş (2021) Novel benzoic acid derivatives: synthesis and biological evaluation as multi-target acetylcholinesterase and carbonic anhydrase inhibitors. Arch Pharm (Weinheim, Ger) 354(3):e2000282. https://doi.org/10.1002/ardp.202000282
28. Türkeş C, Demir Y, Beydemir Ş (2021) Calcium channel blockers: molecular docking and inhibition studies on carbonic anhydrase I and II isoenzymes. J Biomol Struct Dyn 39(5):1672–1680. https://doi.org/10.1080/07391102.2020.1736631
29. Gündoğdu S, Türkeş C, Arslan M, Demir Y, Beydemir Ş (2019) New isoindole-1, 3-dione substituted sulfonamides as potent inhibitors of carbonic anhydrase and acetylcholinesterase: design, synthesis, and biological evaluation. ChemistrySelect 4(45):13347–13355. https://doi.org/10.1002/slct.201903458
30. Istrefi Q, Türkeş C, Arslan M, Demir Y, Nixha AR, Beydemir Ş et al (2020) Sulfonamides incorporating ketene N, S-acetal bioisosteres as potent carbonic anhydrase and acetylcholinesterase inhibitors. Arch Pharm (Weinheim, Ger) 353(6):e1900383. https://doi.org/10.1002/ardp.201900383
31. Sever B, Türkeş C, Altıntop MD, Demir Y, Çiftçi GA, Beydemir Ş (2021) Novel metabolic enzyme inhibitors designed through the molecular hybridization of thiazole and pyrazoline scaffolds. Arch Pharm (Weinheim, Ger) 354(12):e2100294. https://doi.org/10.1002/ardp.202100294
32. Yaşar Ü, Gönül İ, Türkeş C, Demir Y, Beydemir Ş (2021) Transition–metal complexes of bidentate schiff-base ligands: in vitro and in silico evaluation as non-classical carbonic anhydrase and potential acetylcholinesterase inhibitors. ChemistrySelect 29(6):7278–7284. https://doi.org/10.1002/slct.202102082
33. Lolak N, Akocak S, Türkeş C, Taslimi P, Işık M, Beydemir Ş et al (2020) Synthesis, characterization, inhibition effects, and molecular docking studies as acetylcholinesterase, α-glycosidase, and carbonic anhydrase inhibitors of novel benzenesulfonamides incorporating 1, 3, 5-triazine structural motifs. Bioorg Chem. https://doi.org/10.1016/j.bioorg.2020.103897
34. Ellman GL, Courtney KD, Andres V Jr, Featherstone RM (1961) A new and rapid colorimetric determination of acetylcholinesterase activity. Biochem Pharmacol 7(2):88–95. https://doi.org/10.1016/0006-2952(61)90145-9
35. Akocak S, Taslimi P, Lolak N, Işık M, Durgun M, Budak Y et al (2021) Synthesis, characterization, and inhibition study of novel substituted phenylureido sulfaguanidine derivatives as α-glycosidase and cholinesterase inhibitors. Chem Biodivers 18(4):e2000958. https://doi.org/10.1002/cbdv.202000958
36. Taslimi P, Işık M, Türkan F, Durgun M, Türkeş C, Gülçin İ et al (2021) Benzenesulfonamide derivatives as potent acetylcholinesterase, α-glycosidase, and glutathione S-transferase inhibitors: biological evaluation and molecular docking studies. J Biomol Struct Dyn 39(15):5449–5460. https://doi.org/10.1080/07391102.2020.1790422
37. Türkeş C, Akocak S, Işık M, Lolak N, Taslimi P, Durgun M et al (2021) Novel inhibitors with sulfamethazine backbone: synthesis and biological study of multi-target cholinesterases and α-glucosidase inhibitors. J Biomol Struct Dyn. https://doi.org/10.1080/07391102.2021.1916599
38. Çalışkan B, Demir Y, Türkeş C (2021) Ophthalmic Drugs: In vitro paraoxonase 1 inhibition and molecular docking studies. Biotechnol Appl Biochem. https://doi.org/10.1002/bab.2284
39. Tokalı FS, Demir Y, Demircioğlu İH, Türkeş C, Kalay E, Şendil K et al (2022) Synthesis, biological evaluation, and in silico study of novel library sulfonates containing quinazolin-4 (3H)-one derivatives as potential aldose reductase inhibitors. Drug Dev Res 83(3):586–604. https://doi.org/10.1002/ddr.21887
40. Türkeş C, Demir Y, Beydemir Ş (2021) Infection medications: assessment in-vitro glutathione S-transferase inhibition and molecular docking study. ChemistrySelect 6(43):11915–11924. https://doi.org/10.1002/slct.202103197
41. Korkmaz IN, Türkeş C, Demir Y, Öztekin A, Özdemir H, Beydemir Ş (2022) Biological evaluation and in silico study of benzohydrazide derivatives as paraoxonase 1 inhibitors. J Biochem Mol Toxicol. https://doi.org/10.1002/jbt.23180
42. Korkmaz IN, Türkeş C, Demir Y, Özdemir H, Beydemir Ş (2022) Methyl benzoate derivatives: in vitro paraoxonase 1 inhibition and in silico studies. J Biochem Mol Toxicol. https://doi.org/10.1002/jbt.23152
43. Türkeş C, Demir Y, Beydemir Ş (2019) Anti-diabetic properties of calcium channel blockers: inhibition effects on aldose reductase enzyme activity. Appl Biochem Biotechnol 189(1):318–329. https://doi.org/10.1007/s12010-019-03009-x
44. Türkeş C, Kesebir Öztürk A, Demir Y, Küfrevioğlu Öİ, Beydemir Ş (2021) Calcium channel blockers: the effect of glutathione S-transferase enzyme activity and molecular docking studies. ChemistrySelect 6(40):11137–11143. https://doi.org/10.1002/slct.202103100
45. Blois MS (1958) Antioxidant determinations by the use of a stable free radical. Nature 181(4617):1199–1200. https://doi.org/10.1038/1811199a0
46. Re R, Pellegrini N, Proteggente A, Pannala A, Yang M, Rice-Evans C (1999) Antioxidant activity applying an improved ABTS radical cation decolorization assay. Free Radical Biol Med 26(9–10):1231–1237. https://doi.org/10.1016/S0891-5849(98)00315-3
47. Türkeş C, Beydemir Ş, Küfrevioğlu Öİ (2019) In vitro and in silico studies on the toxic effects of antibacterial drugs as human serum paraoxonase 1 inhibitor. ChemistrySelect 4(33):9731–9736. https://doi.org/10.1002/slct.201902424
48. Beydemir Ş, Türkeş C, Yalçın A (2021) Gadolinium-based contrast agents: in vitro paraoxonase 1 inhibition, in silico studies. Drug Chem Toxicol 44(5):508–517. https://doi.org/10.1080/01480545.2019.1620266
49. Işık M, Akocak S, Lolak N, Taslimi P, Türkeş C, Gülçin İ et al (2020) Synthesis, characterization, biological evaluation, and in silico studies of novel 1,3-diaryltriazene-substituted sulfathiazole derivatives. Arch Pharm (Weinheim, Ger) 353(9):e2000102. https://doi.org/10.1002/ardp.202000102
50. Bozdag M, Carta F, Ceruso M, Ferraroni M, McDonald PC, Dedhar S et al (2018) Discovery of 4-hydroxy-3-(3-(phenylureido) benzenesulfonamides as SLC-0111 analogues for the treatment of hypoxic tumors overexpressing carbonic anhydrase IX. J Med Chem 61(14):6328–6338. https://doi.org/10.1021/acs.jmedchem.8b00770
51. Buemi MR, Di Fiore A, De Luca L, Angeli A, Mancuso F, Ferro S et al (2019) Exploring structural properties of potent human carbonic anhydrase inhibitors bearing a 4-(cycloalkylamino-1-carbonyl) benzenesulfonamide moiety. Eur J Med Chem. https://doi.org/10.1016/j.ejmech.2018.11.073
52. Nachon F, Carletti E, Ronco C, Trovaslet M, Nicolet Y, Jean L et al (2013) Crystal structures of human cholinesterases in complex with huprine W and tacrine: elements of specificity for

anti-Alzheimer's drugs targeting acetyl-and butyryl-cholinesterase. Biochem J 453(3):393–399. https://doi.org/10.1042/BJ20130013
53. Türkeş C, Beydemir Ş (2020) Inhibition of human serum paraoxonase-I with antimycotic drugs: in vitro and in silico studies. Appl Biochem Biotechnol 190(1):252–269. https://doi.org/10.1007/s12010-019-03073-3
54. Askin S, Tahtaci H, Türkeş C, Demir Y, Ece A, Çiftçi GA et al (2021) Design, synthesis, characterization, in vitro and in silico evaluation of novel imidazo [2, 1-b][1, 3, 4] thiadiazoles as highly potent acetylcholinesterase and non-classical carbonic anhydrase inhibitors. Bioorg Chem. https://doi.org/10.1016/j.bioorg.2021.105009
55. Türkeş C, Demir Y, Beydemir Ş (2022) Some calcium-channel blockers: kinetic and in silico studies on paraoxonase-I. J Biomol Struct Dyn 40(1):77–85. https://doi.org/10.1080/07391102.2020.1806927
56. Türkeş C (2019) Investigation of potential paraoxonase-I inhibitors by kinetic and molecular docking studies: chemotherapeutic drugs. Protein Pept Lett 26(6):392–402. https://doi.org/10.2174/0929866526666190226162225
57. Demir Y, Türkeş C, Beydemir Ş (2020) Molecular docking studies and inhibition properties of some antineoplastic agents against paraoxonase-I. Anti-Cancer Agents Med Chem 20(7):887–896. https://doi.org/10.2174/1871520620666200218110645
58. Türkeş C, Arslan M, Demir Y, Cocaj L, Nixha AR, Beydemir Ş (2019) Synthesis, biological evaluation and in silico studies of novel N-substituted phthalazine sulfonamide compounds as potent carbonic anhydrase and acetylcholinesterase inhibitors. Bioorg Chem. https://doi.org/10.1016/j.bioorg.2019.103004
59. Işık M, Beydemir Ş, Demir Y, Durgun M, Türkeş C, Nasır A et al (2020) Benzenesulfonamide derivatives containing imine and amine groups: Inhibition on human paraoxonase and molecular docking studies. Int J Biol Macromol. https://doi.org/10.1016/j.ijbiomac.2019.09.237
60. Türkeş C (2019) A potential risk factor for paraoxonase 1: in silico and in-vitro analysis of the biological activity of proton-pump inhibitors. J Pharm Pharmacol 71(10):1553–1564. https://doi.org/10.1111/jphp.13141
61. Kilic A, Beyazsakal L, Işık M, Türkeş C, Necip A, Takım K et al (2020) Mannich reaction derived novel boron complexes with amine-bis(phenolate) ligands: synthesis, spectroscopy and in vitro/in silico biological studies. J Organomet Chem. https://doi.org/10.1016/j.jorganchem.2020.121542
62. Friesner RA, Banks JL, Murphy RB, Halgren TA, Klicic JJ, Mainz DT et al (2004) Glide: a new approach for rapid, accurate docking and scoring. 1. Method and assessment of docking accuracy. J Med Chem 47(7):1739–1749. https://doi.org/10.1021/jm0306430
63. Halgren TA, Murphy RB, Friesner RA, Beard HS, Frye LL, Pollard WT et al (2004) Glide: a new approach for rapid, accurate docking and scoring. 2. Enrichment factors in database screening. J Med Chem 47(7):1750–1759. https://doi.org/10.1021/jm030644s
64. Sever B, Türkeş C, Altıntop MD, Demir Y, Beydemir Ş (2020) Thiazolyl-pyrazoline derivatives: in vitro and in silico evaluation as potential acetylcholinesterase and carbonic anhydrase inhibitors. Int J Biol Macromol. https://doi.org/10.1016/j.ijbiomac.2020.09.043
65. Sever B, Altıntop MD, Demir Y, Türkeş C, Özbaş K, Çiftçi GA et al (2021) A new series of 2,4-thiazolidinediones endowed with potent aldose reductase inhibitory activity. Open Chem. https://doi.org/10.1515/chem-2021-0032
66. Demir Y, Ceylan H, Türkeş C, Beydemir Ş (2021) Molecular docking and inhibition studies of vulpinic, carnosic and usnic acids on polyol pathway enzymes. J Biomol Struct Dyn. https://doi.org/10.1080/07391102.2021.1967195
67. Friesner RA, Murphy RB, Repasky MP, Frye LL, Greenwood JR, Halgren TA et al (2006) Extra precision glide: docking and scoring incorporating a model of hydrophobic enclosure for protein–ligand complexes. J Med Chem 49(21):6177–6196. https://doi.org/10.1021/jm051256o
68. Türkeş C, Arslan M, Demir Y, Çoçaj L, Nixha AR, Beydemir Ş (2022) N-substituted phthalazine sulfonamide derivatives as non-classical aldose reductase inhibitors. J Mol Recognit. https://doi.org/10.1002/JMR.2991
69. Osmaniye D, Türkeş C, Demir Y, Özkay Y, Beydemir Ş, Kaplancıklı ZA (2022) Design, synthesis, and biological activity of novel dithiocarbamate-methylsulfonyl hybrides as carbonic anhydrase inhibitors. Arch Pharm (Weinheim, Ger). https://doi.org/10.1002/ardp.202200132
70. Güleç Ö, Türkeş C, Arslan M, Demir Y, Yeni Y, Hacımüftüoğlu A et al (2022) Cytotoxic effect, enzyme inhibition, and in silico studies of some novel N-substituted sulfonyl amides incorporating 1,3,4-oxadiazol structural motif. Mol Divers. https://doi.org/10.1007/s11030-022-10422-8
71. Pacchiano F, Carta F, McDonald PC, Lou Y, Vullo D, Scozzafava A et al (2011) Ureido-substituted benzenesulfonamides potently inhibit carbonic anhydrase IX and show antimetastatic activity in a model of breast cancer metastasis. J Med Chem 54(6):1896–1902. https://doi.org/10.1021/jm101541x
72. Lou Y, McDonald PC, Oloumi A, Chia S, Ostlund C, Ahmadi A et al (2011) Targeting tumor hypoxia: suppression of breast tumor growth and metastasis by novel carbonic anhydrase IX inhibitors. Cancer Res 71(9):3364–3376. https://doi.org/10.1158/0008-5472.CAN-10-4261
73. Supuran CT, Winum J-Y (2015) Designing carbonic anhydrase inhibitors for the treatment of breast cancer. Expert Opin Drug Discov 10(6):591–597. https://doi.org/10.1517/17460441.2015.1038235
74. Kosak U, Brus B, Knez D, Zakelj S, Trontelj J, Pislar A et al (2018) The magic of crystal structure-based inhibitor optimization: development of a butyrylcholinesterase inhibitor with picomolar affinity and in vivo activity. J Med Chem 61(1):119–139. https://doi.org/10.1021/acs.jmedchem.7b01086
75. Khanfar MA, AbuKhader MM, Alqtaishat S, Taha MO (2013) Pharmacophore modeling, homology modeling, and in silico screening reveal mammalian target of rapamycin inhibitory activities for sotalol, glyburide, metipranolol, sulfamethizole, glipizide, and pioglitazone. J Mol Graph Model. https://doi.org/10.1016/j.jmgm.2013.02.009
76. Riaz S, Khan IU, Bajda M, Ashraf M, Shaukat A, Rehman TU et al (2015) Pyridine sulfonamide as a small key organic molecule for the potential treatment of type-II diabetes mellitus and Alzheimer's disease: in vitro studies against yeast α-glucosidase, acetylcholinesterase and butyrylcholinesterase. Bioorg Chem. https://doi.org/10.1016/j.bioorg.2015.09.008
77. Supuran CT (2016) Structure and function of carbonic anhydrases. Biochem J 473(14):2023–2032. https://doi.org/10.1042/BCJ20160115
78. Neri D, Supuran CT (2011) Interfering with pH regulation in tumours as a therapeutic strategy. Nat Rev Drug Discov 10(10):767–777. https://doi.org/10.1038/nrd3554
79. De Simone G, Alterio V, Supuran CT (2013) Exploiting the hydrophobic and hydrophilic binding sites for designing carbonic anhydrase inhibitors. Expert Opin Drug Discov 8(7):793–810. https://doi.org/10.1517/17460441.2013.795145
80. Littlejohns TJ, Henley WE, Lang IA, Annweiler C, Beauchet O, Chaves PH et al (2014) Vitamin D and the risk of dementia and Alzheimer disease. Neurology 83(10):920–928. https://doi.org/10.1212/WNL.0000000000000755

81. Takeda M, Tanaka T, Okochi M (2011) New drugs for Alzheimer's disease in Japan. Psychiatry Clin Neurosci 65(5):399–404. https://doi.org/10.1111/j.1440-1819.2011.02253.x
82. Tugrak M, Gul HI, Demir Y, Levent S, Gulcin I (2021) Synthesis and in vitro carbonic anhydrases and acetylcholinesterase inhibitory activities of novel imidazolinone-based benzenesulfonamides. Arch Pharm (Weinheim, Ger) 354(4):2000375. https://doi.org/10.1002/ardp.202000375
83. Alyar S, Şen C, Alyar H, Adem Ş, Kalkanci A, Ozdemir UO (2018) Synthesis, characterization, antimicrobial activity, carbonic anhydrase enzyme inhibitor effects, and computational studies on new Schiff bases of Sulfa drugs and their Pd(II), Cu(II) complexes. J Mol Struct. https://doi.org/10.1016/j.molstruc.2018.06.004
84. Mert S, Alım Z, İşgör MM, Anıl B, Kasımoğulları R, Beydemir Ş (2019) Novel pyrazole-3, 4-dicarboxamides bearing biologically active sulfonamide moiety as potential carbonic anhydrase inhibitors. Arab J Chem 12(8):2740–2748. https://doi.org/10.1016/j.arabjc.2015.05.020
85. Rice-Evans CA, Miller NJ, Paganga G (1996) Structure–antioxidant activity relationships of flavonoids and phenolic acids. Free Radical Biol Med 20(7):933–956. https://doi.org/10.1016/0891-5849(95)02227-9
86. Durgun M, Türkeş C, Işık M, Demir Y, Saklı A, Kuru A et al (2020) Synthesis, characterisation, biological evaluation and in silico studies of sulphonamide Schiff bases. J Enzyme Inhib Med Chem 35(1):950–962. https://doi.org/10.1080/14756366.2020.1746784

Authors and Affiliations

Nebih Lolak[1] · Süleyman Akocak[1] · Mustafa Durgun[2] · Hatice Esra Duran[3] · Adem Necip[4] · Cüneyt Türkeş[5] · Mesut Işık[6] · Şükrü Beydemir[7,8]

✉ Nebih Lolak
nlolak@adiyaman.edu.tr

✉ Cüneyt Türkeş
cuneyt.turkes@erzincan.edu.tr

[1] Department of Pharmaceutical Chemistry, Faculty of Pharmacy, Adıyaman University, 02040 Adiyaman, Turkey

[2] Department of Chemistry, Faculty of Arts and Sciences, Harran University, 63290 Şanlıurfa, Turkey

[3] Department of Medical Biochemistry, Faculty of Medicine, Kafkas University, 36100 Kars, Turkey

[4] Department of Pharmacy Services, Vocational School of Health Services, Harran University, 63300 Şanlıurfa, Turkey

[5] Department of Biochemistry, Faculty of Pharmacy, Erzincan Binali Yıldırım University, 24002 Erzincan, Turkey

[6] Department of Bioengineering, Faculty of Engineering, Bilecik Şeyh Edebali University, 11230 Bilecik, Turkey

[7] Department of Biochemistry, Faculty of Pharmacy, Anadolu University, 26470 Eskişehir, Turkey

[8] The Rectorate of Bilecik Şeyh Edebali University, 11230 Bilecik, Turkey